NASA

Technical Memorandum 80560

Microscale Instabilities in Stream Interaction Regions

Aharon Eviatar
Melvyn L. Goldstein

AUGUST 1979

National Aeronautics and
Space Administration

Goddard Space Flight Center
Greenbelt, Maryland 20771

MICROSCALE INSTABILITIES IN STREAM INTERACTION REGIONS

Aharon Eviatar
Department of Geophysics and Planetary Sciences
Tel-Aviv University
Ramat-Aviv, Israel

Melvyn L. Goldstein
Laboratory for Extraterrestrial Physics
NASA-Goddard Space Flight Center
Greenbelt, Maryland 20771

Submitted to: The Journal of Geophysical Research

ABSTRACT

A theoretical investigation of the microstructure of solar wind stream interaction regions is presented. We discuss the role of several electrostatic kinetic instabilities which may be important within the stream interface and the compression region. Inside of 1 AU the interface is likely to be stable against the electrostatic streaming instabilities considered. Between 1 and 2 AU we argue that the interface will excite the magnetized ion-ion instability. The compression region is also found to be unstable beyond 1 AU where the modified two-stream instability, beam-cyclotron instability, and ion-acoustic instability will be important in determining the structure of the compressive pulses as they evolve into forward and reverse shocks. We conclude that the modified two-stream instability and beam-cyclotron instability predominately play a role in heating the electrons to the threshold for the ion-acoustic instability. Various electrostatic plasma waves, ranging in frequency from the lower-hybrid to harmonics of the electron cyclotron frequency, would be produced by these instabilities. Their signature should also be seen by high time resolution measurements of the temperature of the various plasma species.

1. INTRODUCTION

Two prominant features of the interaction regions of high and low speed solar wind streams are the stream interface and the surrounding compression region which, at distances beyond 1 AU, often evolves into forward and reverse shock pairs. In both these regions there is observational and theoretical evidence suggesting that strong gradients form in solar wind velocity, plasma density and/or magnetic field. In this paper, we examine the consequences of assuming that as the scale lengths of the gradients decrease both the stream interface and compression region will excite several electrostatic instabilities.

In the following section we first investigate the stream interface, and argue that ions from the fast stream are likely to penetrate at least an ion Larmor radius into the slow stream, thereby exciting the magnetized ion-ion instability. The region in the heliosphere where this instability can be excited is restricted by the necessity for there to be a fairly large (≥20 km s^{-1}) discontinuous jump in the component of solar wind velocity orthogonal to the interplanetary magnetic field. This is most likely to first occur near 1 AU or slightly beyond. The wave modes excited, their frequency, and the effect of the instability on the temperatures of the electrons, protons and helium are discussed.

In §3 a similar discussion is developed for the compression region. There too, we argue that the plasma is likely to become unstable as the forward and reverse shocks begin to form. The electron-ion instabilities excited there will produce a wide range of electrostatic waves, ranging in frequency from the lower-hybrid to harmonics of the electron gyrofrequency. Estimates are given for the saturation amplitudes of these instabilities, and their role in limiting the thickness of the developing shock structure.

2. STREAM INTERFACES

<u>Observations.</u> A stream interface is a sharp transition in velocity, density, temperature and flow angle of the wind often observed within the stream interaction region. It separates the cool dense slow stream from the hot tenuous fast stream and is associated with a local maximum in thermal pressure [for a review see Burlaga, 1975]. The existence of a tangential discontinuity separating the fast and slow streams was suggested as early as 1963 [v., e.g. Dessler and Fejer, 1963].

Interfaces were first reported by Belcher and Davis [1971] based on three-hour average data. Subsequently Burlaga [1974] showed that interfaces could be very thin although he also included fairly broad interfaces where the transitions in flow velocity and density took ~30 minutes, but these will not concern us. The existence of large jumps in flow velocity at stream interfaces appears confined to observations near 1 AU. Beyond 2 AU Pioneers 10 and 11 did not usually observe such discontinuities [see, e.g. Smith and Wolfe, 1977]. The kinetic effects discussed below can only be important at those interfaces which exhibit sharp, discontinuous changes in flow velocity over the fastest time scales available to plasma instruments. One should keep in mind, however, that the time interval over which those measurements have traditionally been made is still long compared with the few tenths of a second that it takes a region of a few ion Larmor radii to be convected past a spacecraft. Additional observations have been reported by Gosling et al. [1978] who analyzed the properties of the flow near 23 discontinuous interfaces with thicknesses less than 4×10^4 km. These were observed only when the solar wind speed was less than 450 km s^{-1}. They further found evidence of a sharp shear flow in solar wind velocity at interfaces, and noted that at interfaces the electron temperature rose sharply there by about 40%. We will argue below that several of these features are a natural consequence of kinetic instabilities operating in regions of sharp gradients in plasma velocity and density.

Because of the very high conductivity of the solar wind it is difficult for material on neighboring magnetic flux tubes to interpenetrate. Consequently, as fast plasma overtakes slow plasma, a compression region forms which tends to steepen with increasing heliocentric distance, eventually forming a tangential discontinuity separating the compressed ambient plasma from the fast stream [Hundhausen, 1972, p. 132ff; Hundhausen and Burlaga, 1975]. If this boundary becomes as thin as a few proton Larmor radii, the faster stream can begin to penetrate the slower one. It is at this stage that kinetic effects become important. Inside of ~0.3 AU, where adjoining flux tubes are nearly radial, the only kinetic interaction allowed is a viscous shear [e.g. Eviatar and Wolf, 1968]. By the time the streams have reached 0.5 AU, however, the component of the velocity jump across the interface perpendicular to $\underline{B}$ can exceed the thermal velocity of solar wind protons. This situation can then be unstable to excitation of an electrostatic instability known as the magnetized ion-ion instability (MII), provided that $2V_i < U \cdot \sin(\Gamma) < 2.5(1+\beta_e)V_A$, where U is the magnitude of the velocity change at the interface, $\Gamma \equiv \Omega_s R/V_{SW}$ is the (garden-hose) angle at heliocentric distance R between the radius vector and the magnetic line of force, $\Omega_s = 2.7 \times 10^{-6}$ is the angular rotation rate of the sun, $\beta_e \equiv 8\pi NT_e/B^2$ is the ratio of electron thermal energy density to magnetic energy density, T_e

is the electron temperature, $V_A \equiv B(4\pi NM)^{-1/2}$ is the Alfvén speed, N is the total density in the interpenetration region of the two streams, V_{SW} is the solar wind velocity in the <u>slow</u> stream, M is the ion mass, and V_i is the ion thermal velocity [Papadopoulos et al., 1971]. The geometry of the interaction is shown in Figure 1.

<u>The Magnetized Ion-Ion Instability.</u> This instability has been investigated in a somewhat different context with regard to the stream interaction in papers by Papadopoulos [1973a] and Papadopoulos et al. [1974]. Our application of the magnetized ion-ion instability to the stream interaction problem differs in several respects. Papadopoulos [1973a], following Papadopoulos et al. [1971], simplified the dispersion relation for the MII by assuming that the ions were cold, <u>i.e.</u> $V_i \ll \omega/k \sim U$. In addition, as noted above, U must be less than a few times V_A. In the solar wind V_i is often of order V_A and these two conditions are difficult to satisfy simultaneously. This has necessitated a return to the more general dispersion relation in which the ions are warm. From the studies of Burlaga [1974] and Gosling et al. [1978], we know that discontinuous jumps in the solar wind velocity observed at 1 AU are typically only 15-50 km s^{-1}; and even with a jump of 50 km s^{-1} the component directed across $\underline{B}$ is reduced by a factor of $\sin\Gamma$. In this situation the plasma is very close to marginal stability and the warm ion dispersion relation must be used.

Furthermore, Papadopoulos [1973a] and Papadopoulos et al. [1974] assumed that even close to the sun the plasma flowed across $\underline{B}$ [cf. Figure 1a in Papadopoulos, 1973a]. But to date there is no observational evidence in support of such an initial condition. It is interesting to note, however, that the interaction regions of streams do appear sharper at smaller heliocentric distances [Rosenbauer et al., 1977], although the scale of the velocity gradients remains larger than required for interpenetration. The assumption that gradients associated with stream interactions should be steeper near the sun than at 1 AU was used in the multifluid simulations reported by Papadopoulos et al. [1974], and was implicit in the kinetic calculations of Goldstein and Eviatar [1973] and Papadopoulos [1973a]. Recently, evidence has been presented indicating that the interface itself is not necessarily a discontinuity inside ~0.6 AU [Schwenn, Mühlhäuser, and Marsch, 1978]. In the following discussion we adopt the picture illustrated in Figure 1 in which the fast stream originates in regions of the corona adjacent to those giving rise to slow flow; as would occur at coronal holes. Thus close to the corona the flow is initially characterized by a shear in velocity, and only at distances greater than 0.6 AU will the component of velocity across $\underline{B}$ exceed $2V_i$.

In deriving the dispersion relation for the MII we have retained terms which arise from electromagnetic and finite β_e effects because in the solar wind those terms can be important [Wagner et al., 1971].

The properties of the magnetized ion-ion instability can be found from the general dispersion relation for waves propagating at a large angle to $\underline{B}$ [Stix, 1962]. In the appropriate regime of unmagnetized ions but magnetized electrons, the general dispersion relation simplifies greatly. These simplifications are justified so long as the growth rate, γ, exceeds Ω_i=eB/Mc, the thermal ion Larmor frequency (M is the proton mass), which in turn requires that the wavenumber, k, satisfy $L_i^{-1} << k << L_e^{-1}$, where $1/L_{i,e} = \Omega_{i,e}/V_{i,e}$, and where L_i (L_e) is the thermal ion (electron) Larmor radius, and $\Omega_e=|eB/mc|$ (m is the electron mass). The sums over Bessel functions appearing in the general dispersion relation can then be eliminated. The frequency range is thus restricted to $\Omega_i^2 << |\omega|^2 << \Omega_e^2$, where ω is the complex frequency of the oscillation. We retain the warm electron term in order to investigate the validity of the usual assumption that the waves propagate so nearly perpendicular to $\underline{B}$ that $\omega/(kV_e \sin\theta) >> 1$, where $\tan\theta \equiv k_{||}/k_{\perp}$.

With these assumptions the dispersion relation for the magnetized ion-ion instability in the frame of the slow plasma becomes (Appendix A)

$$\frac{\alpha\omega_i^2}{2k^2V_i^2} Z'\left(\frac{\omega - kU\sin(\Gamma)\cos(\theta)}{\sqrt{2}kV_i}\right) + \frac{(1-\alpha)\omega_i^2}{2k^2V_i^2} Z'\left(\frac{\omega}{\sqrt{2}kV_i}\right) \cdot$$

$$\frac{\omega_e^2}{2k^2V_e^2} \frac{Z'\left(\frac{\omega}{\sqrt{2}kV_e\sin(\theta)}\right)}{\left[1+\frac{\omega_e^2}{k^2c^2(1+\beta_e)}\right]} = 1 + \frac{\omega_e^2}{\Omega_e^2}\left[1 + \frac{\omega_e^2}{k^2c^2(1+\beta_e)}\right] \qquad (2.1)$$

where $\omega_{i,e}^2 \equiv 4\pi Ne^2/(M,m)$, $T_e \equiv mV_e^2$, and α is the fractional density in each stream. As pointed out by McBride and Ott [1972], in reference to the related modified two-stream instability, electromagnetic effects ($\omega_e^2/k^2c^2 \neq 0$) can sometimes have a stabilizing influence. In the solar wind, because $L_i/L_e \sim 20$ one has $\omega_e^2/k^2c^2 \gtrsim 1$ and the electromagnetic corrections cannot be ignored. Observations indicate [Burlaga, 1974 and Gosling et al., 1978] that at stream interfaces the faster plasma is about half as dense as the slow material, and so we have taken $\alpha = 1/3$. Equation (2.1) can then be solved numerically. The existence of unstable roots depends sensitively on the variation of solar wind parameters throughout the interplanetary medium.

Close to the sun, where $U \cdot \sin\Gamma/V_i << 1$, no instability is found. As one moves out in heliocentric distance to about 0.8 AU, $U \cdot \sin\Gamma/V_i \geq 1$ and excitation of the magnetized ion-ion instability depends primarily on the local values of U, V_i, and V_{SW}. We have investigated solutions to (2.1) extending from 0.6 AU to 5 AU using a range of values for solar wind parameters. Because the MII excites waves propagating perpendicular to $\underline{B}$, it is $(T_i)_\perp$ which controls the onset of the instability, and so we have used $T_i = (T_i)_\perp = 2$ eV (2×10^4 °K) in (2.1) at 1 AU. For N and $\underline{B}$ (also at 1 AU) we took $N=7cm^{-3}$ and $\underline{B}=5\times10^{-5}$ G. To evaluate (2.1) at heliocentric distances both larger and smaller than 1 AU, we adopted the following scaling laws: $N(R)\sim1/R^2$, $T_i(R) \sim R^{-(4/3)}$, and $T_e(R) \sim R^{-(1/3)}$ [see, e.g. the discussion in Hundhausen, 1972 and the recent measurements by Ogilvie and Scudder, 1978]. To determine the variation in the threshold conditions of the magnetized ion-ion instability we varied V_{SW} from 250 km s^{-1} to 450 km s^{-1} using the T-V relation [Burlaga and Ogilvie, 1973], $\sqrt{T_i} \propto V_{SW}$. This was normalized so that $(T_i)_\perp = 2$ eV for $V_{SW} = 350$ km s^{-1}.

As an example, consider the solution to (2.1) at 1.5 AU with $V_{SW} = 300$ km s^{-1}. Using the 1 AU values and the scaling relations defined above, we found unstable roots to (2.1) when the discontinuous jump in velocity at the interface was U = 40 km s^{-1}. [Recall that U denotes the total jump in V_{SW} at the interface--the component perpendicular to $\underline{B}$ is $U \cdot \sin\Gamma(R)$]. In Figure 2, we have plotted the real and imaginary roots, $\omega(k,\theta)$ and $\gamma(k,\theta)$ first against θ using the value of k which maximizes γ at each θ (denoted k_m) and then against k using the value of θ which maximizes γ at each k (denoted θ_m). γ is plotted for two different values of β_e. Figure 2a illustrates the well known property of the MII that it is most efficiently excited across the magnetic field. Note that for $\theta < 1°$, we could have assumed that the electrons were "cold" and expanded the electron plasma dispersion function [Papadopoulos, 1973a]. The effect of making such a cold electron approximation is illustrated in Figure 3 (using somewhat different parameters). The cold electron approximation is seen to be valid only so long as $\theta < 1°$.

From Figure 2, we can define $\gamma_m \equiv \gamma(k_m, \theta_m)$ as the maximum value of γ, maximized with respect to both k and θ. In Figure 4, we have plotted γ_m and ω_m [the value of $\omega(k,\theta)$ associated with γ_m] against R using two different values of U and a wind velocity of V_{SW} = 300 km s^{-1}. Also plotted in the Figure is Ω_i and ω_o defined by

$$\omega_o^2 \equiv \frac{\omega_i^2}{[1+(\omega_e^2/\Omega_e^2)]} \tag{2.2}$$

In the solar wind because $\omega_e^2/\Omega_e^2 >> 1$, $\omega_o \approx \omega_{LH} \equiv \sqrt{\Omega_e \Omega_i}$. Papadopoulos et al. [1971] found that γ_m was as large as ω_o. However, because of the stabilizing effects of the electromagnetic contributions to (2.1), together with the fact that U is not much greater than V_i, we find that γ_m is systematically smaller than ω_o, but that $\omega_m \approx \omega_o$, as it is in the cold ion approimation. (Note that our definition of ω_o differs by a factor of $\sqrt{2}$ from that of Papadopoulos et al. [1971].) For U = 50 km s^{-1} the magnetized ion-ion instability is first excited at 1 AU, while for U = 40 km s^{-1} threshold for the MII is not reached until 1.5 AU. This reflects the distance at which U$\cdot$sinΓ first exceeds V_i by an amount sufficient to excite the instability. Our assumption that the ions are demagnetized is verified <u>a posteriori</u> because $\gamma_m > \Omega_i$.

The heliocentric distance at which the MII is likely to reach threshold is a sensitive function of U and V_{SW}. This relationship is shown in Figure 5, where U is plotted against R for various values of V_{SW}. The curves represent the values of R and U for which γ_m exceeds Ω_i, and suggest the heliocentric distance at which the MII is likely to become important. For example, for discontinuous velocity jumps of 40 km s^{-1} in a 250 km s^{-1} solar wind (recall that V_{SW} refers to the slow stream), the MII can be excited at 1 AU and beyond. However, if the "slow" wind has a velocity of 450 km s^{-1}, then with U=40 km s^{-1} the MII is not likely to be excited inside 2 AU. In general, the smaller the velocity jump and the higher the wind speed, the further out one must go before the conditions for excitation of the MII can be satisfied. However, even U $\approx$ 20 km s^{-1} is adequate to excite the MII near 2 AU with V_{SW} $\approx$ 250-300 km s^{-1}. Conversely, velocity jumps in excess of 40 km s^{-1} are necessary in order to excite the MII inside 1 AU. Thus this instability is likely to be important where V_{SW} is low and U ~ 20-40 km s^{-1}.

Saturation Effects. The nonlinear stages of the magnetized ion-ion instability have been intensively investigated both theoretically and by means of computer simulations [Papadopoulos et al., 1971]. The waves first evolve as described by quasilinear theory until ion trapping becomes important. Stabilization then occurs after a time $\tau_M \equiv (M/eE^*k)^{1/2} \approx 1/\gamma_m$ (E^* is the rms value of the electric field of the growing wave [Manheimer, 1971]). Subsequently, the ions are reflected in the potential wells of the waves and the waves will stop growing after being further amplified by another factor of e = 2.7 [Papadopoulos et al., 1971]. From the definition of τ_M the maximum value of the electric field is

$$E_M = [8\pi(2.7)Mc^2N]^{1/2} (k_m c/\omega_i) (\gamma_m/k_m c)^2 \quad (2.3)$$

In Figure 6 we have plotted E_M between 1 and 5 AU for V_{SW}=300 km s^{-1} and U=50 km s^{-1}. Values lie are between 100-400 μV/m with the peak occurring near 2 AU. Observation of these waves has thus far not been reported, perhaps because the frequency range is below that of most experiments that have been flown. For example, on Helios 1 and 2 where $\omega_{LH}/2\pi < 10$ Hz the plasma wave experiment was insensitive below 31 Hz [Gurnett and Anderson, 1977]. The waves may be difficult to detect because the instability occurs over only a few ion Larmor radii ($L_i \sim 50$ km at 1 AU), a distance which is convected past a spacecraft in less than a second.

Stabilization by ion trapping suggests that within the interface the ion temperature should be significantly enhanced over its value on either side. In essence, within the stabilization region the thermal velocity will have increased to $\sim [V_i + U \cdot \sin(\Gamma)]$, so that as long as $U \cdot \sin\Gamma \geq 2V_i$ the increase in temperature can exceed a factor of two. Computer simulations in which $U \cdot \sin\Gamma >> V_i$ have found that the ion temperature at stabilization is $T_i \sim 0.3M_i[U \cdot \sin\Gamma]^2$ [Papadopoulos, 1973a], with the increase being primarily in $(T_i)_\perp$. Gosling et al. [1978] using one-hour averages reported an increase of nearly a factor of two in $(T_i)_\perp$ at the interface (cf. their Figure 4). With five-minute averages only the change in $(T_i)_{||}$ was reported [v. Figure 2 of Gosling et al., 1978]. Of course, enhancements in T_i caused by kinetic interactions are in addition to those expected due to the compression of the solar wind fluid at the interface and those resulting from the different boundary conditions in the coronal source regions of the fast and slow streams.

Alpha particles will also be affected by the MII. Once thermalized, the alpha particle temperature will be of order $T_\alpha \sim (M_\alpha/2) \cdot (U \cdot \sin\Gamma)^2$, so that $(T_\alpha/T_i) \approx (M_\alpha/M) = 4$. Gosling et al. [1978] only report one-hour averages of alpha particle parameters near interfaces, and so their observations may primarily reflect fluid, as opposed to kinetic, characteristics of the stream interaction. Nonetheless, they found that at interfaces the alpha to proton temperature ratio increased by more that 30%, and that T_α itself rose by nearly a factor of three.

One additional consequence of this instability is that at the interface the amount of shear at the tangential discontinuity will be reduced because the primary effect of the ion trapping is to thermalize that component of the flow directed across $\underline{B}$, i.e. the fraction $(1/2)M(U \cdot \sin\Gamma)^2$. It is important to realize that the instability does not convert all of the streaming energy into electrostatic waves. In fact, for the values of E_M shown in Figure 6, only a very small fraction of the streaming energy ($< 10^{-6} MU^2$) is converted into waves in the process of thermalizing the ions and producing the increase in proton temperature at the interface. Because the component of the flow parallel to $\underline{B}$ is unaffected, the directed flow of the fast plasma appears to change from radial to shear at an interface. At greater heliocentric distances a larger fraction of the flow energy will be thermalized by the instability, E_m will increase, and the shear should decrease until the instability has eroded the velocity gradients to the point where it cannot be excited. In this context it is not surprising that discontinuous jumps in velocity are often absent in interfaces observed beyond 1 AU.

Electron Heating. At first glance the magnetized ion-ion instability would not appear to be a very efficient means of heating electrons. However, the electrons will respond to the electrostatic fields produced by the ion-ion interaction by drifting in the direction of $\underline{E}\times\underline{B}$ [Papadopoulos et al., 1971]. For electric fields approaching 1 mV/m, the drift velocity can exceed 100 km s^{-1}, which is adequate, as we shall discuss in more det' l in the next section, to excite the modified two-stream instabil' y. his instability both heats the electrons, increasing $(T_e)_{||}$, and lowers U_e, their mean drift velocity. The primary source of free energy is the electron drift energy $(1/2)mU_e^2$ [Lampe et al., 1975]. Assuming that $U_e \approx$ 200km s^{-1}, and $V_e \approx 1000$ km s^{-1}, the increase in perpendicular electron temperature at the interface will be ~5%. Gosling et al. [1978] utilizing five-minute averaged data do report an increase in $(T_e)_{||}$ of some 10% at interfaces (v. their Figure 3).

In the following section we examine several kinetic interactions which may be important in the formation of the forward and reverse shocks often observed in stream interaction regions beyond 1 AU.

3. FORWARD AND REVERSE SHOCKS

The compression region on either side of the stream interface steepens with heliocentric distance until a forward and reverse shock pair forms (see Fig. 1). These corotating shock pairs have not been observed inside 1 AU [Rosenbauer et al., 1977], and are only rarely observed at 1 AU [Ogilvie, 1972]. However, when Pioneer 10 and 11 encountered corotating stream interaction regions beyond 1 AU, observation of shock pairs became common [Smith and Wolfe, 1977]. Pizzo [1978a] and [1978b], using multidimensional fluid models of corotating streams, has shown that formation of forward and reverse shock pairs is expected to occur only near and beyond 1 AU. Nonradial flows in these models transport mass, energy and momentum away from the compression region and that tends to delay the formation of shocks to beyond 1 AU.

In this section we discuss several microinstabilities likely to be excited as the forward and reverse shocks form in the compression region. The instabilities considered are not meant to exhaust all possibilities, and for example we consider neither the closely related lower-hybrid drift instability [Davidson et al., 1977], nor the drift-cyclotron instability [Gladd and Huba, 1979]. The ones treated do, however, illustrate the range of frequencies and classes of waves that one might observe with appropriate instrumentation.

Modified Two-Stream Instability (MTSI). As the compressive MHD waves steepen, the local magnetic gradients within the waves produce streaming of electrons through ions. This situation was first described by Fredricks

[1969]. In a plasma in which $T_e < 10T_i$ this streaming is known to excite the modified two-stream instability [Ott et al., 1972 and McBride et al., 1972]. This instability is similar to the magnetized ion-ion instability discussed above; the major distinction is that instead of having two ion distributions flowing through each other in the presence of electrons, one now has a single ion distribution streaming through electrons. The MTSI can be excited so long as V_d, the relative velocity of electrons and ions, exceeds both V_i and the sound speed, $C_s \equiv (T_e/M)^{1/2}$. Again we retain the electromagnetic corrections to the dispersion relation, allow both the ion and electrons distributions to be warm, and restrict our attention to the wavenumber and frequency range $L_i^{-1} \ll k \ll L_e^{-1}$ and $\Omega_i^2 \ll |\omega|^2 \ll \Omega_e^2$, respectively. The resulting dispersion relation becomes (Appendix A)

$$-\frac{\omega_i^2}{2k^2V_i^2} Z'\left(\frac{\omega - kV_d\cos(\theta)}{\sqrt{2}kV_i}\right) + \frac{\omega_e^2}{2k^2V_e^2} \frac{Z'\left(\dfrac{\omega}{\sqrt{2}kV_e\sin(\theta)}\right)}{\left[1 + \dfrac{\omega_e^2}{k^2c^2(1+\beta_e)}\right]} = 1 + \frac{\omega_e^2}{\Omega_e^2}\left[1 + \frac{\omega_e^2}{k^2c^2(1+\beta_e)}\right] \tag{3.1}$$

Excitation of the instability is determined by the magnitude of V_d, which in turn is determined by the drift current, J_e, within the MHD wave. Thus [Fredricks, 1969]

$$c(\Delta B/\Delta x) = 4\pi J_e = 4\pi NeV_d \tag{3.2}$$

We solve (3.1) using V_d as a free parameter. Once having found the value of V_d which maximizes the growth rate, (2.2) can be used to estimate the scale size of the MHD wave required to excite the MTSI. Because the growth rates are relatively insensitive to V_{SW} and R, we first solve (3.1) using parameters typical of 1 AU; a choice which permits comparison with the results of Lemons and Gary [1977], who have used a more general formulation of the MTSI to investigate the formation and structure of the earth's bow shock.

In Figure 7 we plot the real and imaginary roots of (3.1) first versus k [at the value of θ which maximizes $\gamma(k)$], and then versus θ [at the value of k which maximizes $\gamma(\theta)$]. The computations were performed using V_{SW} = 450 km s^{-1}, R = 1 AU, $T_i = (T_i)_\perp$ = 3.3 eV, B = 5 γ, N = 7 cm^{-3}, and β_e = 0.6 and 1.1. In this example, $V_d = 5V_i$. As illustrated in the Figure, as β_e decreases, γ_m increases as more free energy becomes available to drive the instability, i.e. $V_d - C_s$ increases. In deriving (3.1) it was necessary to assume that $k_{||}/k < V_d/V_e$ in order to reduce to a single term the summations over electron Bessel functions which appear in the full dispersion relation. This implies that the validity of (2.1) is restricted to the domain $\theta < 4°$ (with β_e=1.1) or $\theta < 5°$ (for β_e=0.6). In contrast, Lemons and Gary [1977] retained the sums over Bessel functions and found that although $\gamma(k_m,\theta)$ was still maximum at small values of θ, it remained relatively constant to beyond $\theta < 20°$. (Note that our definition of θ is the complement of the definition used by Lemons and Gary [1977].) Figure 8 shows γ_m and ω_m for the modified two-stream instability as a function of V_d/V_i for β_e=1.1 and 0.6 (T_e = 10 and 5 ev, respectively). At threshold $V_d \approx 3-4V_i$ and $\omega_m \ll \omega_{LH}$. As V_d increases, so does γ_m, while ω_m increases more rapidly, eventually exceeding ω_{LH}.

As mentioned above, the scale of the MHD pulse can be estimated from (3.2), now rewritten in a more convenient form:

$$\Delta x \approx \left(\frac{\Omega_e}{\omega_e}\right)\cdot\left(\frac{c}{V_d}\right)\cdot\left(\frac{\Delta B}{B}\right)\cdot\left(\frac{c}{\omega_e}\right) \tag{3.3}$$

At 1 AU we have $\Omega_e/\omega_e = 5.9\times10^{-3}$. Assuming $V_d/V_i \approx 3$ at threshold, $c/V_d \approx 8.4\times10^3$, so that $\Delta x = 150(c/\omega_{pe}) \approx 300$ km for $\Delta B/B = 3$. This value for Δx is consistent with observational and theoretical evidence of thicknesses of large amplitude MHD waves and shocks [see, e.g. Fredricks and Coleman, 1969 and Manheimer and Boris, 1972].

The situation at 2 AU is similar, and is also illustrated in Figure 8. Again the instability threshold is reached at $V_d/V_i \approx 3$-4, and $\Delta x \approx 92(c/\omega_e) \approx 370$ km, where now $\Omega_e/\omega_e = 5\times10^{-3}$, $\Delta B/B = 3$, $N=1.75$ cm^{-3}, $(T_i)_\perp = 1.3$ eV and $V_{SW} = 450$ km s^{-1}. This value for Δx is close to the thicknesses of ~1000 km reported by Smith and Wolfe [1977] for forward and reverse shock pairs using 453 km s^{-1} as the average propagation speed.

Saturation Effects. The modified two-stream instability results in heating both ions and electrons. The unmagnetized ions are primarily heated by raising $(T_i)_\perp$, while the electrons, constrained as they are to move along $\underline{B}$, are primarily heated in $(T_e)_{||}$ [Ott et al., 1972]. Stabilization of the MTSI has been studied using numerical simulations [Ott et al., 1972 and McBride et al., 1972] where trapping was found to be the stabilization mechanism. Waves propagating at angles $\theta > (m/M)^{1/2} \approx 1.3°$ trapped electrons, while ion trapping occurred first if $\theta < (m/M)^{1/2}$. From Figure 7, significant growth is obtained only for $\theta_m < 1.3°$, so that ion trapping is likely to be the more important effect. Consequently, (2.3) can be used to estimate the magnitude of the electric fields associated with this instability, and we find that for $V_d/V_i \simeq 4$ at both 1 and 2 AU, and $E \simeq 100\ \mu V/m$ which increases to $\simeq 300\ \mu V/m$ when $V_d/V_i \simeq 8$-10. If the MTSI evolves to saturation, V_d would be reduced to the marginally stable level ($V_d/V_i \simeq 3$-4) and an amount of free energy equal to $(1/2)Nm \cdot (\Delta V_d)^2$ could be extracted from the current and converted to wave energy and heating [Lampe et al., 1975]. The amount of electron heating that actually occurs depends sensitively on ΔV_d; ranging from as much as a 10% increase in $(T_e)_{||}$ if $\Delta V_d \simeq 8\ V_i$, to a negligible change in $(T_e)_{||}$ if $\Delta V_d \simeq V_i$.

The modified two-stream instability is not the only cross-field instability that can be excited in MHD pulses. Several others produce electrostatic waves at frequencies well above ω_{LH}, and thus may be more easily observable by plasma-wave experiments. We will briefly consider two such instabilities; the beam-cyclotron and the ion-acoustic instabilities.

Beam-cyclotron instability. Like the modified two-stream, the beam cyclotron instability (also known as the electron cyclotron drift instability) is driven by a relative drift of electrons and ions. In this case the instability arises from a coupling of Bernstein and ion acoutic waves [Forslund et al., 1970 and Gary and Sanderson, 1970]. The resulting unstable waves are confined to a narrow cone about the normal to $\underline{B}$ (as are Bernstein waves) with frequencies close to harmonics of Ω_e, and $kL_e > 1$ [Gary, 1971]. To excite the instability, V_d must exceed C_s. Significant growth occurs even with $T_e \simeq T_i$ and $\beta_e \simeq 1$ [Lashmore-Davies, 1971]. This instability has been extensively studied both analytically and in numercial simulations by Lampe et al. [1972].

The dispersion relation for $\mathbf{k}\cdot\mathbf{B}=0$ and $kL_e>1$ has been derived by Lampe et al. [1972], and is given by

$$1 - (k\lambda_e)^{-2}\cdot(T_e/T_i)\cdot Z'\left(\frac{\omega-kV_d}{\sqrt{2}kV_i}\right) + (k\lambda_e)^{-2} + (k\lambda_e)^{-2}\,\frac{\omega}{2\sqrt{2}kV_e}\,\cdot$$

$$\{Z\left(\frac{\omega}{\sqrt{2}kV_\rho}\right) - Z\left(\frac{-\omega}{\sqrt{2}kV_e}\right) + i\cdot\cot(\pi\omega/\Omega_e)\cdot[Z\left(\frac{\omega}{\sqrt{2}kV_e}\right) + Z\left(\frac{-\omega}{\sqrt{2}kVe}\right)]\} \tag{3.4}$$

where $\lambda_e=v_e/\omega_e$ is the electron Debye length, and $\mathbf{V}_d$ is assumed parallel to $\mathbf{k}$. The neglect of electromagnetic effects in (3.4) is well justified for the parameter range of interest [Lampe et al., 1972]. Because of the strong Landau damping of Bernstein waves propagating at $\theta\neq0$, the unstable waves are similarly confined to angles $\theta<\Omega_e/(2\pi\omega_e k_\perp\lambda_e)$ [Kamimura et al., 1978]. At 1 AU, $\omega_e/\Omega_e\simeq170$, so that $\theta<1°$ for $k\lambda_e\simeq0.1$. For a given frequency, unstable solutions to (3.4) are somewhat sensitive to the ratio of V_d/V_i--large V_d results in smaller $k\lambda_e$, and hence a wider propagation zone.

To compare properties of this instability with the MTSI we solved (3.4) using solar wind parameters typical of 1 AU with $\beta_e=1.1$. As in Figure 8, $V_{SW}=450$ km s^{-1}, $N=7$ cm^{-3}, $B=5$ γ, and $T_e/T_i=3$. The results are shown in Figure 9 for $V_d/V_i=10$, where γ and ω are plotted as functions of k for the first 8 harmonics of Ω_e. The maxima in γ, denoted γ_m, fall approximately at

$$k = \frac{n\Omega_e}{V_d - C_s/(1 + k^2\lambda_e^2)^{1/2}} \tag{3.5}$$

a relationship derived by Lampe et al. [1972] for the case $T_e>>T_i$. Although the ratio γ_m/ω is rather small, ranging from 5×10^{-3} - 5×10^{-2}, γ_m is 5-6 times greater than found for the MTSI (cf. Figure 8). On the other hand, the beam-cyclotron instability requires a slightly higher threshold for V_d (5-6 V_i, compared to 3-4 V_i for the MTSI). Thus it is not altogether clear which instability will dominate, although one can imagine a situation in which the MTSI is first excited, but is not immediately able to dissipate the available free energy. The MHD waves will then continue to steepen, and V_d will increase until the beam-cyclotron instability is excited. Once excited, because of its large growth rate, the beam-cyclotron instability will saturate before the MTSI. The quasilinear and nonlinear stages of evolution have been examined by Lampe et al. [1972] who found that initially the beam-cyclotron instability saturated at a relatively low level via resonance-broadening. Once this happened, they found that the plasma could be further unstable to the ion-acoustic instability because the nonlinear dispersion relation for the beam-cyclotron instability when saturated through resonance-broadening has the form of the <u>linear</u> zero magnetic field ion-acoustic dispersion relation. In the solar wind, where T_e/T_i is usually too low to excite the ion-acoustic instability, the beam-cyclotron instability will saturate, allowing the modified two-stream instability to evolve until ion or electron trapping has reduced V_d to a marginally stable state. However, because both the MTSI and beam cyclotron instabilities can heat electrons at least to some extent, it is quite possible that T_e will increase by just enough to excite the ion-acoustic instability. We explore this possibility below.

In spite of the consensus that saturation of the beam-cyclotron instability via resonance broadening occurs at a low level of electric field turbulence [Lampe et al., 1972; Biskamp, 1973 and Lemons and Gary, 1978], it is not clear that this will be true for solar wind parameters. The ci cal amplitude of the turbulent fields when resonance broadening becomes important was found by Lampe et al. [1972] to be $E \approx 96 \cdot [NT_e(\Omega_e/\omega_e)^3(1/k\lambda_e)]^{1/2}$ (mV/m), with T_e measured in eV. Assuming $N \approx 7$ cm^{-3}, $k\lambda_e \approx 5\times10^{-2}$, and $\omega_e/\Omega_e \approx 170$, we find $E \approx 1$ mV/m, which is actually larger than the value of $\sim$100 μV/m found above for the saturation level of the modified two-stream instability.

From our numerical solutions of (3.4), we know that the instability can be excited up to at least the eleventh harmonic of Ω_e, the exact maximum being a function of V_d/V_e [Lampe et al., 1972]. These high harmonics have relatively large values of $k\lambda_e$, and are thus confined to a very narrow cone about $\theta \approx 0$ of much less than 1°. This may in turn limit the growth of the highest harmonics because of the necessity of the magnetic field to remain constant in direction over a growth time [Lemons and Gary, 1978]. These waves have frequencies in the range 100-1000 Hz, depending on the amount of Doppler shift, and should be easily observable. In fact, Wu and Fredricks [1972] have argued that this instability may have been observed in the earth's bow shock where amplitudes of 1-20 mV/m have been reported at frequencies near 1 kHz [Fredricks et al., 1970; Fredricks and Coleman, 1969]. Biskamp's [1973] suggestion that the observed turbulence levels were too high to be explained by the beam-cyclotron instability should be reexamined, at least for space plasmas.

The quasilinear analysis and numerical simulations carrried out by Lampe et al. [1972] indicate that as long as $V_d \gg C_s$, the bulk of the energy taken out of the relative streaming between the protons and electrons goes into heating electrons. Thus the beam-cyclotron instability appears to be more efficient at heating electrons than is the modified two-stream instability, and with $V_d = 10V_i \approx 6C_s$, electron heating should be fairly efficient. At that drift velocity, only a small fraction of the total available free energy (equal to MV_d^2) need go into electron heating in order that the electron temperature increase substantially. For example, T_e would double if an amount of energy equal to $MV_d^2/30$ were removed from the stream. Again, based on the results of Lampe et al. [1972], this is probably the maximum amount of energy that could be extracted before saturation by ion trapping occurs. Even this amount is unlikely unless the beam-cyclotron instability in turn excites the ion-acoustic instability. Therefore it is of interest to see just how much it is necessary to heat the electrons before excitation of the ion-acoustic instability becomes possible.

Ion-Acoustic Instability. The threshold for the ion-acoustic instability can be found from the dispersion relation discussed by Fried and Gould [1961] and Stringer [1964]. In our notation:

$$1 - (1/2k^2\lambda_e^2)\cdot(T_e/T_i)\cdot Z'\left(\frac{\omega-kV_d}{\sqrt{2}kV_i}\right) - (1/2k^2\lambda_e^2)\cdot Z'\left(\frac{\omega}{\sqrt{2}kV_e}\right) = 0 \qquad (3.6)$$

For $V_d/V_i = 10$, unstable roots first appear at $T_e/T_i \approx 10$. Recall we have assumed that initially $(T_e)_{||}/(T_i)_{\perp} \approx 3$. As we have seen, an increase in T_e/T_i by more than a factor of two is highly unlikely. If the ion-acoustic instability is not excited, relatively little streaming energy will be removed from the plasma. Therefore, the MHD pulse, or shock will continue to evolve, causing V_d to increase still further. As V_d/V_i approaches 20, it is then possible to excite the ion-acoustic instability with $(T_e)_{||}/(T_i)_{\perp} \approx 6$.

The ion-acoustic instability saturates by ion trapping [Biskamp and Chodura, 1971 and Lampe et al., 1972], and is capable of reducing the relative streaming to maginally stable levels. As an example, in Figure 10 we have plotted ω and γ against k for the case V_d/V_i = 20 and T_e/T_i = 7. These waves too will be subject to a Doppler shift in the solar wind, but should be observable by plasma wave instruments currently flown. [Note that because we have assumed that the protons are streaming through stationary electrons, the values of ω in Fig. 9 can exceed ω_i and $\omega/k>C_s$.] Saturated turbulent field intensities of order 1 mV/m can be expected. Furthermore, the ion-acoustic instability produces waves propagating into a wide cone about θ=0. In fact, for $V_d/V_i \approx 20$, $\Delta\theta \approx 80°$.

4. CONCLUSIONS

In the preceeding sections we have discussed several kinetic instabilities which we argue are important in determining the microscale structure of the solar wind stream interaction region. The selected instabilities are not meant to comprise an exhaustive list. We have ignored, for example, all of the lower-hybrid drift instabilities driven by strong gradients in density and magnetic field, primarily because their physics is similar in many respects to the magnetized ion-ion and modified two-stream instabilities [v., e.g. Lemons and Gary, 1978]. Another example of a related instability we did not discuss is the cross field, current driven ion-acoustic instability [Barrett et al., 1972] because this shares many characteristics with the field free instability and MTSI.

Perhaps the best way to summarize our discussion is to imagine following a stream interaction region as it evolves outward in the interplanetary medium. If one assumes that the fast stream originates in a coronal hole, while the slower material comes from the adjoining region, then close to the sun a shear interaction will predominate. Although we have not discussed any kinetic instabilities in this region, one can imagine several dynamical effects which might be important. For example, if the gradients in the shear become so large that the fast and slow ions are separated by only a few Larmor radii, then an electromagnetic ion cyclotron instability would be excited if the shear velocity exceeded $\sim 2.7V_A$ [Eviatar and Wolf, 1968 and Goldstein and Eviatar, 1973]. On a larger scale the interface could become Kelvin-Helmholtz unstable. Eventually, however, the interface between the two streams will steepen as the faster flow begins to overtake the slower

(v. Fig. 1). At the interface the flow can be thought of as having two components, one along the interface, parallel to the magnetic field, the other across the field. Because of their large gyroradii, the ions will be the first component of the fast stream to penetrate the slow plasma. Depending primarily on the relative velocities of the two streams and the velocity of the solar wind in the slow flow, this situation will become unstable to the magnetized ion-ion instability somewhere between 1 and 2 AU. The magnetized ion-ion instability will heat the ions (proportional to their mass). The amplified electric fields produced by the interpenetration of the two streams can then give rise to $\underline{E} \times \underline{B}$ drifts which excite either the modified two-stream instability or one of the other instabilities discussed in §2. Excitation of these kinetic instabilities will quickly erode any sharp gradients at the interface, leaving it in a state of marginal stability.

Beyond one AU the compression region, which has gradually steepened as the streams evolve, forms pulses within which strong gradients in $\underline{B}$ can excite various electron-ion cross field instabilities. The possible range of frequencies excited extends from the lower-hybrid (due to the modified two-stream instability) through the ion-acoustic frequency range, to harmonics of the electron cyclotron frequency. It appears unlikely that either the modified two-stream instability or the beam-cyclotron instability would be able to reduce the streaming to a marginally stable state. Should that be the case, the compression regions would continue to evolve until those two instabilities had heated the electrons sufficiently to drive ion-acoustic waves unstable. Once excited, the observed shock thickness and electron temperature would remain close to their marginally stable level

[Manheimer and Boris, 1972]. As yet, insufficient research has been conducted on the detailed structure of forward and reverse shocks in stream interaction regions to know whether the structure is consistent with this scenario. However, Morse and Greenstadt [1976], in an analysis of the earth's bow shock, did conclude that under certain conditions the thickness of the shock appear to be controlled by the conditions for marginal stability against the ion-acoustic instability. Present and future plasma wave experiments on deep space probes should be able to answer many of these questions.

APPENDIX

The dispersion relation can be written in the form:

$$\underline{E}^{*}\cdot\underline{D}\cdot\underline{E} = 0 \tag{A1}$$

where $\underline{D}$ is the dyadic given by Montgomery and Tidman [1961 eq. 10.35]. It is convenient to write the electric field as the sum of electrostatic and electromagnetic waves:

$$\underline{E} = -i[\phi\underline{k} + (\omega/c)\,\underline{A}] \tag{A2}$$

where ϕ and $\underline{A}$ are the scalar electrostatic and vector electromagnetic vector potentials, respectively. We take $\underline{B}_o$ in the $\hat{\underline{z}}$ direction, $\underline{k} = (k_\perp, 0, k_{||})$, and $\underline{A} = A\hat{\underline{y}}$. Expansion of (A1) gives

$$\phi^2[k_\perp^2\, D_{xx} + k_{||}k_\perp(D_{xz} + D_{zx}) + k_{||}^2\, D_{zz}] + (\omega/c)^2\, A^2\, D_{yy}$$

$$+ \phi\, A\, (\omega/c)\, k_{||}\, (D_{yz} + D_{zy}) = 0 \tag{A3}$$

where we have used $D_{xy} = -D_{yx}$.

Following McBride et al. [1972], we assume $\Omega_i << |\omega| << |\Omega_e|$, $k_{||} << k_\perp$, $k^2L_e{}^2 << 1$, and $k^2L_i{}^2 >> 1$, which implies that the ion trajectories are well approximated by straight lines and the electron trajectories by helicies. We also assume that the temperatures of each species are the same in both streams and are isotropic. However, the ion and electron temperatures may differ from on another.

For the magnetized ion-ion instability we take the following distribution functions

$$f_i = \frac{1}{(2\pi)^{3/2}V_i^3} \quad \alpha \exp[-(\underline{v} - \underline{U})^2/2V_i^2] + (1-\alpha) \exp[-v^2/2V_i^2]$$

$$f_e = \frac{1}{(2\pi)^{3/2}V_e^3} \exp(-v^2/2V_e^2) \tag{A4}$$

where $\underline{U} = (U\sin\Gamma, 0, U\cos\Gamma)$ is the drift velocity and Γ is the garden-hose angle.

Let ψ be the angle between $\underline{k}$ and $\underline{U}$, and θ the angle between $\underline{k}$ and the normal to $\underline{B}$. Then the ion component of the electrostatic dispersion relation, which is the part of (A3) multiplying Φ^2, becomes

$$1 - \frac{\omega_i^2}{2k^2V_i^2} \alpha Z'\left(\frac{\omega - k \cdot u}{\sqrt{2}kV_i}\right) + (1 - \alpha) Z'\left(\frac{\omega}{\sqrt{2}kV_i}\right)$$

where $Z(\zeta) \equiv (1/\sqrt{\pi}) \int_{-\infty}^{\infty} dy \exp(-y^2)/(y - \zeta)$ is the plasma dispersion function. Using $\psi + \theta + \Gamma = \pi/2$, and $\sin\theta \approx 0$, we have

$$\underline{k} \cdot \underline{U} = k\ U \cos\psi = k\ U\ (\sin\Gamma \cos\theta + \cos\Gamma \sin\theta)$$

$$= k\ U \sin(\Gamma + \theta) \approx k\ U \sin\Gamma \cos\theta.$$

This provides the ion terms of equation (2.1).

The electrons, on the other hand, are highly magnetized. In the strong magnetic field limit, the electrostatic electron terms become

$$\frac{\omega_e^2}{k^2V_e^2}\{1 - \exp(-k^2L_e^2)\, I_o(k^2L_e^2)\, [1 + (1/2)Z'(\omega/\sqrt{2}kV_e\sin\theta)]\}$$

I_o is the modified Bessel function.

The electromangetic and mixed terms proportional to A^2 and ϕA in (A3) tend to stabilize these instabilities, and so must be kept [McBride et al., 1972]. However, in the range of frequencies of interest here, it is possible to further simplify these terms by taking the fluid limit in which all resonances are ignored. Thus we take the arguments of the Bessel functions to be small, the arguments of the plasma dispersion functions to be large (except for n = 0) and expand accordingly. We also use $I_0' = I_1$, $I_o \approx 1 + (1/4)\cdot(kV_e/\Omega_e)^4$, and $I_1 \approx (1/2)\cdot(kV_e/\Omega_e)^2$. We retain the warm electron terms for reasons discussed in the text and obtain terms of the type

$$1 + \frac{(\omega_e/kc)^2}{1 + \beta_e + \omega_e/kc}\, Z'(\omega/\sqrt{2}kV_e\sin\theta) + (\omega_e/\Omega_e)^2 \cdot\ 1 + \frac{\omega_e/kc}{1 + \beta_e}$$

Combining these terms gives (2.1). If we replace the ion distribution function given in (A4) by

$$f_i = \frac{1}{(2\pi)^{3/2}V_i^3}\exp[-(\underline{v} - \underline{V}_D)^2/2V_i^2]$$

we obtain the dispersion relation for the modified two-stream instability given in (3.1).

Acknowledgements. We would like to thank Drs. J. S. Scudder, L. Burlaga, A. Klimas and K. Ogilvie for many stimulating discussions. One of us (A. E.) acknowledges the support provided by the Department of Physics and Astronomy of the University of Maryland and the Laboratory for Extraterrestrial Physics of the Goddard Space Flight Center during the summers of 1977 and 1978, when this work was performed.

REFERENCES

Barrett, P. J., B. D. Fried, C. F. Kennel, J. M. Sellen, and R. J. Taylor, Cross-field current-driven ion-acoustic instability, Phys. Rev. Lett., 28, 337, 1972.

Belcher, J. W., and L. Davis, Jr., Large-amplitude Alfvén waves in the interplanetary medium, 2, J. Geophys. Res., 76, 3534, 1971.

Biskamp, D., Collisionless shock waves in plasmas, Nucl. Fusion, 13, 719, 1973.

Biskamp, D., and R. Chodura, in Plasma Physics and Controlled Nuclear Fusion Research (Proc. 4th Int. Conf. Madison, 1971) 2, IAEA, Vienna, p. 265ff, 1971.

Burlaga, L. F., Interplanetary stream interfaces, J. Geophys. Res., 79, 3717, 1974.

Burlaga, L. F., Interplanetary streams and their interaction with the earth, Space Sci. Rev., 17, 327, 1975.

Burlaga, L. F., and K. W. Ogilvie, Solar wind temperature and speed, J. Geophys. Res., 78, 2028, 1973.

Davidson, R. C., N. T. Gladd, and C. S. Wu, Effects of finite plasma beta on the lower-hybrid-drift instability, Phys. Fluids, 20, 301, 1977.

Dessler, A. J., and J. A. Fejer, Interpretation of K_p index and M-region geomagnetic storms, Planet. Space Sci., 11, 505, 1963.

Eviatar, A., and R. A. Wolf, Transfer processes in the magnetopause, J. Geophys. Res., 73, 5561, 1968.

Forslund, D. W., R. L. Morse, and C. W. Nielson, Electron cyclotron drift instability, Phys. Rev. Lett., 25, 1266, 1970.

Fredricks, R. W., Electrostatic heating of solar wind ions beyond 0.1 AU, *J. Geophys. Res.*, *74*, 2919, 1969.

Fredricks, R. W., and P. J. Coleman, Jr., Observations of the microstructure of the earth's bow shock, in *Proc. Intern. Conf. on Plasma Instabilities in Astrophysics*, edited by D. G. Wentzel and D. A. Tidman, pp. 199-228, Gordon and Breach, New York, 1969.

Fredricks, R. W., G. M. Crook, C. F. Kennel, I. M. Green, F. L. Scarf, P. J. Coleman, and C. T. Russell, OGO-5 observations of electrostatic turbulence in bow shock magnetic structures, *J. Geophys. Res.*, *75*, 3751, 1970.

Fried, B. D., and R. W. Gould, Longitudinal ion oscillations in a hot plasma, *Phys. Fluids*, *4*, 139, 1961.

Gary, S. P., Longitudinal waves in a perpendicular collisionless plasma shock. Part 3. $T_e \sim T_i$, *J. Plasma Phys.*, *6*, 561, 1971.

Gary, S. P., and J. J. Sanderson, Longitudinal waves in a perpendicular collisionless plasma shock, I, Cold ions, *J. Plasma Phys.*, *4*, 739, 1970.

Gladd, N. T. and J. D. Huba, Finite beta effects on the drift-cyclotron instability, *Phys. Fluids*, *22*, 911, 1979.

Goldstein, M. L., and A. Eviatar, Turbulent heating of colliding streams in the solar wind, *The Astrophy. J.*, *179*, 627, 1973.

Gosling, J. T., J. R. Asbridge, S. J. Bame, and W. C. Feldman, Solar wind stream interfaces, *J. Geophys. Res.*, *83*, 1401, 1978.

Gurnett, D. A., and R. R. Anderson, Plasma wave electric fields in the solar wind: initial results from Helios 1, *J. Geophys. Res.*, *83*, 632, 1977.

Hundhausen, A. J., *Coronal Expansion and Solar Wind*, Springer-Verlag, New York, 1972.

Hundhausen, A. J., and Burlaga, L. F., A model for the origin of solar wind stream interfaces, J. Geophys. Res., 80, 1845, 1975.

Kamimura, T., T. Wagner, and J. M. Dawson, Simulation study of Bernstein modes, Phys. Fluids, 21, 1151, 1978.

Lampe, M., W. M. Manheimer, and K. Papadopoulos, Anomalous transport coefficients for HANE applications due to plasma micro-instabilities, Memorandum Report 3076, Naval Research Laboratory, Washington, D. C., 1975.

Lampe, M., W. M. Manheimer, J. B. McBride, J. H. Orens, K. Papadopoulos, R. Shanny, and R. N. Sudan, Theory and simulation of the beam cyclotron instability, Phys. Fluids, 15, 662, 1972.

Lashmore-Davies, C. N., Instability in a perpendicular collisionless shock wave for arbitrary ion temperatures, Phys. Fluids 14, 1481, 1971.

Lemons, D. S., and S. P. Gary, Electromagnetic effects on the modified two-stream instability, J. Geophys. Res., 82, 2337, 1977.

Lemons, D. S., and S. P. Gary, Current-driven instabilities in a laminar perpendicular shock, J. Geophys. Res., 83, 1625, 1978.

Manheimer, W. M., Strong turbulence theory of nonlinear stabilization and harmonic generation, Phys. Fluids, 14, 579, 1971.

Manheimer, W. M., and J. P. Boris, Self-consistent theory of a collisionless resistive shock, Phys. Rev. Lett., 28, 659, 1972.

McBride, J. B., and E. Ott, Electromagnetic and finite β_e effects on the modified two stream instability, Phys. Lett., 39A, 363, 1972.

McBride, J. B., E. Ott, J. P. Boris, and J. H. Orens, Theory and simulation of turbulent heating by the modified two-stream instability, Phys. Fluids, 15, 2367, 1972.

Montgomery, D. C., and D. A. Tidman, Plasma Kinetic Theroy, McGraw-Hill, New York, 1964.

Morse, D. L., and E. W. Greenstadt, Thickness of magnetic structures associated with the earth's bow shock, J. Geophys. Res., 81, 1791, 1976.

Ogilvie, K. W., Corotating shock structures, in Solar Wind, edited by C. P. Sonett, P. J. Coleman, Jr., and J. M. Wilcox, NASA SP-308, Washington, D. C., 1972.

Ogilvie, K. W., and J. D. Scudder, The radial gradients and collisional properties of solar wind electrons, J. Geophys. Res., 83, 3776, 1978.

Ott, E., J. B. McBride, J. H. Orens, and J. P. Boris, Turbulent heating in computer simulations of the modified plasma two-stream instability, Phys. Rev. Lett., 28, 88, 1972.

Papadopoulos, K., Electrostatic turbulence at colliding plasma streams as the source of ion heating in the solar wind, The Astrophys. J., 179, 931, 1973a.

Papadopoulos, K., Nonthermal turbulent heating in the solar envelope, The Astrophys. J., 179, 939, 1973b.

Papadopoulos, K., R. W. Clark, and C. E. Wagner, Simulation of colliding solar wind streams with multifluid codes, in Solar Wind Three, edited by C. T. Russell, Institute of Geophysics and Planetary Physics, University of California, Los Angeles, 1974.

Papadopoulos, K., R. C. Davidson, J. M. Dawson, I. Haber, D. A. Hammer, N. A. Krall, and R. Shanny, Heating of counterstreaming ion beams in an external magnetic field, Phys. Fluids, 14, 849, 1971.

Pizzo, V., A three-dimensional model of corotating streams in the solar wind 1. Theoretical foundations, J. Geophys. Res., 83, 5563, 1978a.

Pizzo, V., An evaluation of corotating solar wind stream models, in Contributions to the Fourth Solar Wind Conference, Technical Memorandum 79711, NASA-Goddard Space Flight Center, Greenbelt, Maryland, 1978b, to be published in Solar Wind IV.

Rosenbauer, H., R. Schwenn, E. Marsch, B. Meyer, H. Miggenrieder, M. D. Montgomery, K. H. Mühlhäuser, W. Pilipp, W. Voges and S. M. Zink, A survey on initial results of the Helios plasma experiment, J. Geophys., 42, 561, 1977.

Schwenn, R., K. H. Mühlhäuser, E. Marsch, and H. Rosenbauer, Solar wind stream structure between 0.3 and 1 AU at the time of solar activity minimum, to be published in Solar Wind IV.

Smith, E. J., and J. H. Wolfe, Pioneer 10, 11 observations of evolving solar wind streams and shocks beyond 1 AU, in Study of Travelling Interplanetary Phenomena 1977, edited by M. A. Shea, D. F. Smart and S. T. Wu, pp. 227-257, D. Reidel, Dordrecht-Holland, 1977.

Stix, T. H., The Theory of Plasma Waves, McGraw-Hill, New York, 1962.

Stringer, T. E., Electrostatic instabilities in current-carrying and counterstreaming plasmas, J. Nuc. Energy (Part C), 6, 267, 1964.

Wagner, C. E., K. Papadopoulos, and I. Haber, Electromagnetic and finite β_e effects on the counterstreaming ion instability, Phys. Letters, 35A, 440, 1971.

Wu, C. S., and R. W. Fredricks, Cyclotron drift instability in the bow shock, J. Geophys. Res., 77, 5585, 1972.

FIGURE CAPTIONS

Fig. 1. Schematic view of the stream interaction region showing the compression (shaded) and rarefaction produced as high velocity plasma (long arrows) overtakes the low velocity plasma. The view is onto the ecliptic plane from above the north pole. The spiral pattern of the magnetic field is also shown. For further datails see Pizzo [1979a], from which this figure is adapted.

Fig. 2. Growth rate γ, and real frequency ω, of the magnetized ion-ion instability (eq. 1.1) at 1.5 AU. In panel (a), ω and γ are plotted against θ, the angle between $\underline{k}$ and the normal to $\underline{B}$, with $|\underline{k}|$ held constant, and equal to k_m, the value which maximizes $\gamma(k)$. In panel (b), the wavenumber variation of ω and γ are shown with $\theta=\theta_m$, the value which maximizes $\gamma(\theta)$. Note that the maximum value of γ is relatively insensitive to variations in β_e, although the angular spread of γ is greatly reduced as β_e decreases. Because ω is relatively insensitive to variations in β_e, only $\omega(\beta_e=0.9)$ is plotted. In computing these values of ω and γ we used $V_{SW}=300$km s^{-1} and 1 AU values of T_i and N equal to 2 eV and 7 cm^{-3}, respectively. The scaling laws defined in the text were employed to find T_i and N at 1.5 AU. In addition, we used U=40 km s^{-1}, where UsinΓ is the component of the velocity jump in V_{SW} at the interface that is perpendicular to $\underline{B}$.

Fig. 3. The dashed curve represents a solution to (1.1) for the magnetized ion-ion instability in which the electron plasma dispersion function was approximated using the asymptotic expansion valid for large argument, or

equivalently, small electron thermal velocity. That approximation is seen to be valid only for very small angles ($\lesssim 1°$), at least for parameters typical of the solar wind. In this example, the 1 AU values of U, V_{SW}, T_i and β_e were 50 km s^{-1}, 300 km s^{-1}, 1.5 eV and 1.9, respectively. The solution was obtained at R=2AU. T_i(1 AU) and β_e(1 AU) were found from the assumed radial dependence discussed in the text.

Fig. 4. A plot of ω_m and γ_m as functions of heliocentric distance, with V_{SW}=300 km s^{-1}. γ_m is the maximum growth rate of the magnetized ion-ion instability, maximized with respect to both k and θ; ω_m is the accompanying value of $\omega(k_m, \theta_m)$. Results are plotted using both U=40 and 50 km s^{-1}. Also plotted is $\omega_o(R)$, given by (1.2), and $\Omega_i(R)$. Note that $\gamma_m > \Omega_i$, justifying the assumption that the ions are unmagnetized. The largest values of γ_m are found between 1 and 2 AU.

Fig. 5. The threshold conditions of the magnetized ion-ion instability plotted as a function of U and R for three different values of V_{SW}. The magnetized ion-ion instability is unstable for values of U which lie above the curve corresponding to the choice of V_{SW}.

Fig. 6. The maximum value of the electric field in lower-hybrid waves excited by the magnetized ion-ion instability. Stabilization is assumed to occur by ion trapping. The largest values of E are found between 1.5-2.5 AU. The curve was obtained using V_{SW}=300 km s^{-1}, and U=50 km s^{-1}.

Fig. 7. In panel (a), $\gamma(k, \theta_m)$, the growth rate of the modified two-stream

instability, is plotted as a function of k for β_e=0.6 and 1.1 at $\theta=\theta_m$. In panel (b), k is held constant at $k=k_m$, and γ is plotted against θ. In both panels V_{SW}=450 km s^{-1}, R= 1 AU, T_i=3.3 eV, B=5 γ, and N=7 cm^{-3}. In addition, $\omega(k,\theta_m)$ and $\omega(k_m,\theta)$ are shown for β_e=1.1.

Fig. 8. Real and imaginary frequencies of the modified two-stream instability as a function of V_d/V_i. Solid lines represent the solution at 1 AU using N=7 cm^{-3}, and $(T_i)_\perp$=3.3 eV. Dashed lines represent the solution at 2 AU using N=1.75 cm^{-3}, and $(T_i)_\perp$=1.3 eV. In both cases V_{SW}=450 km s^{-1}. The solution for ω_m is shown for β_e=1.1 at 1 AU and β_e=1.5 at 2 AU, while γ_m is also plotted for β_e(1 AU)=0.6 and β_e(2 AU)=0.8. The variation in N, T_i, and β_e between 1 and 2 AU is a result of the scaling with heliocentric distance discussed in §1.

Fig. 9. Real and imaginary roots of the dispersion relation for the beam-cyclotron instability as functions of kL_e (bottom scale), and $k\lambda_e$ (top scale). The parameters are characteristic of 1 AU (N=7 cm^{-3}, B=5 γ, T_e/T_i=3, β_e=1.1). In addition, V_{SW}=450 km s^{-1} and V_d/V_i=10.

Fig. 10. Solution of the ion-acoustic dispersion relation assuming V_d/V_i=20 and T_e/T_i=7. As before N=7 cm^{-3} and V_{SW}=450 km s^{-1}.

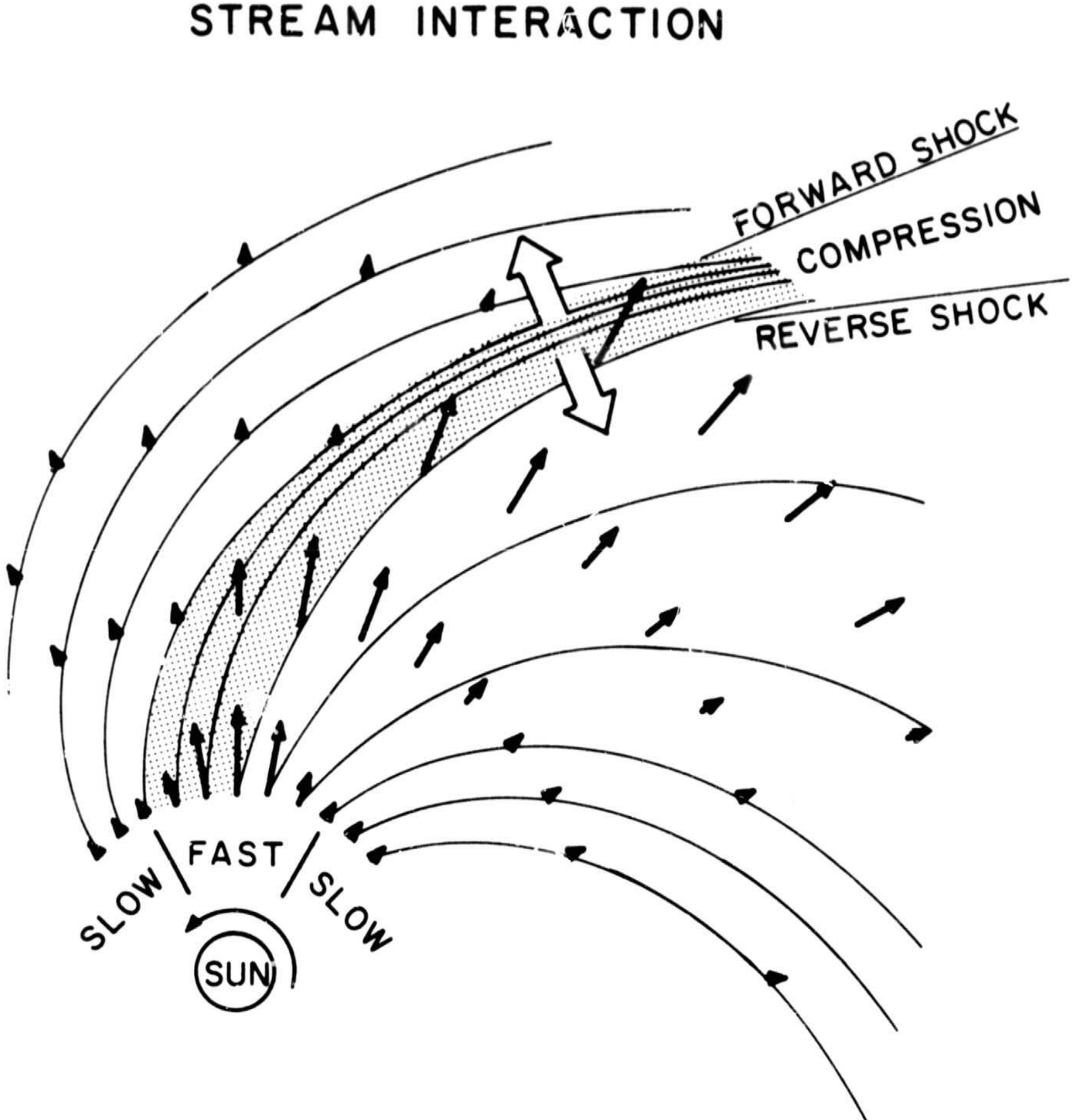
STREAM INTERACTION
FORWARD SHOCK
COMPRESSION
REVERSE SHOCK
SLOW
FAST
SLOW
SUN

Figure 1

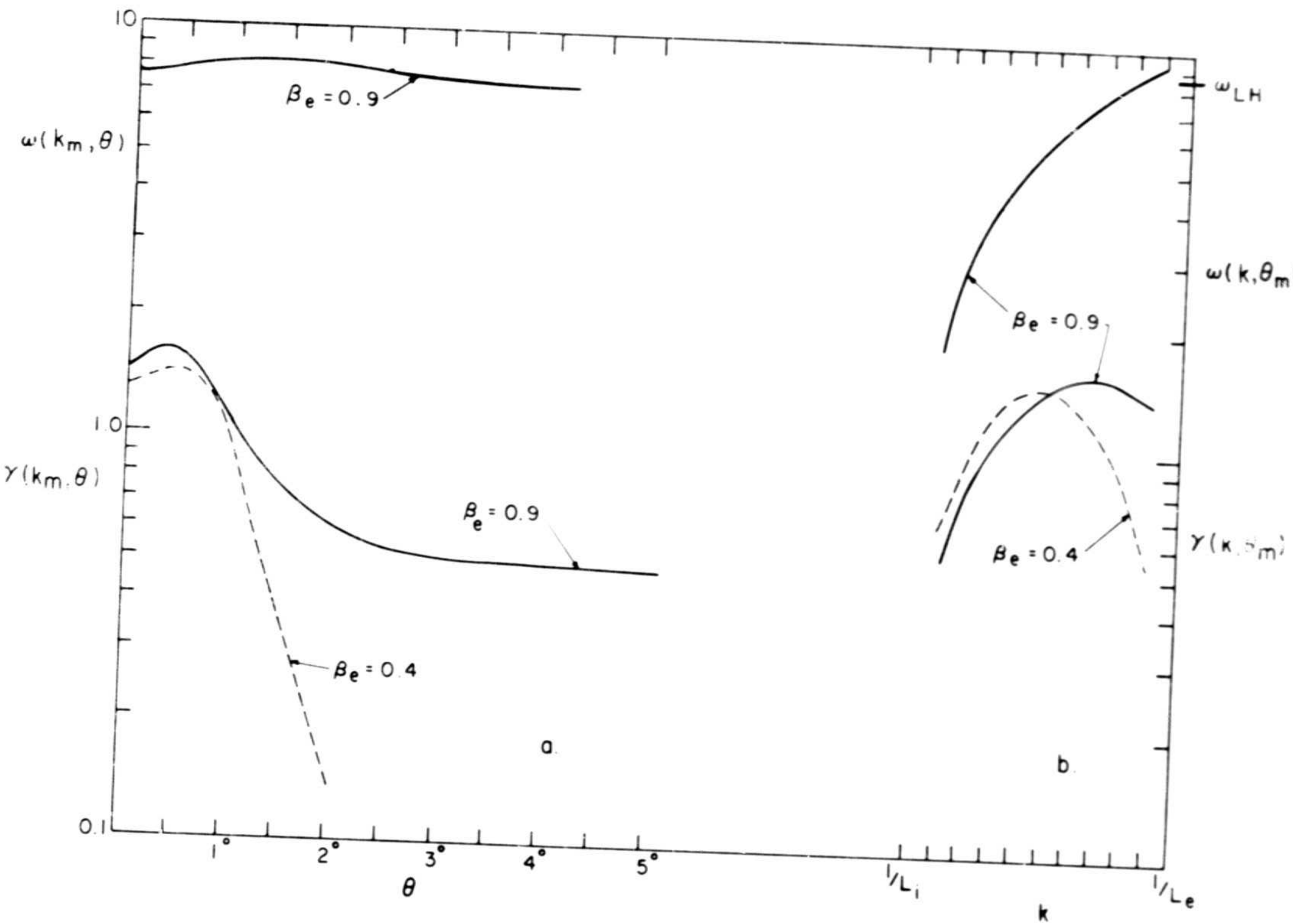

10
1.0
0.1
ω(k_m, θ)
γ(k_m, θ)
β_e = 0.9
β_e = 0.9
β_e = 0.4
a
1°
2°
3°
4°
5°
θ
ω_LH
ω(k, θ_m)
β_e = 0.9
β_e = 0.4
b
1/L_i
k
1/L_e

Figure 2

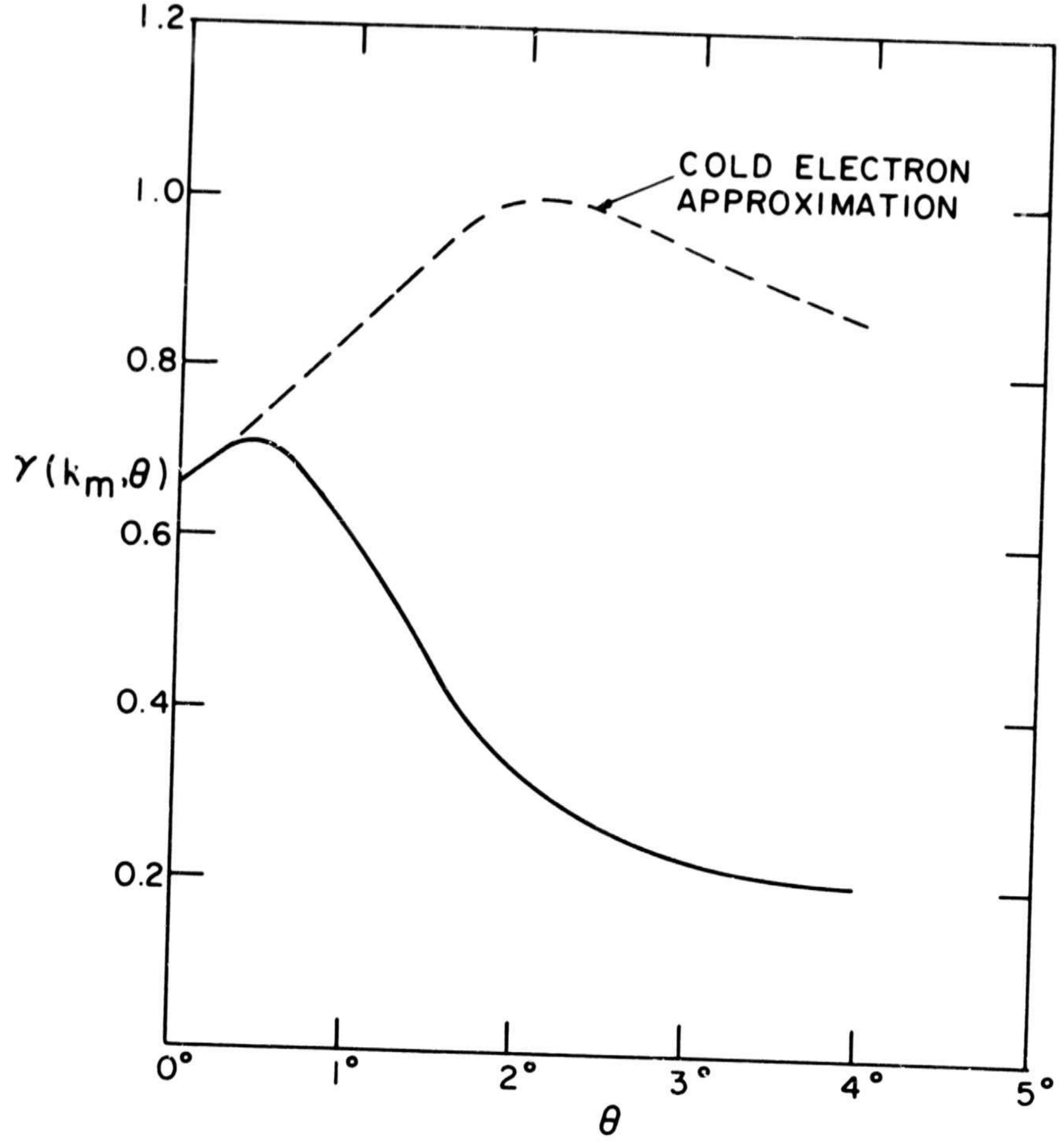

1.2
1.0
0.8
0.6
0.4
0.2
COLD ELECTRON APPROXIMATION
$\gamma(k_m, \theta)$
0°
1°
2°
3°
4°
5°
θ

Figure 3

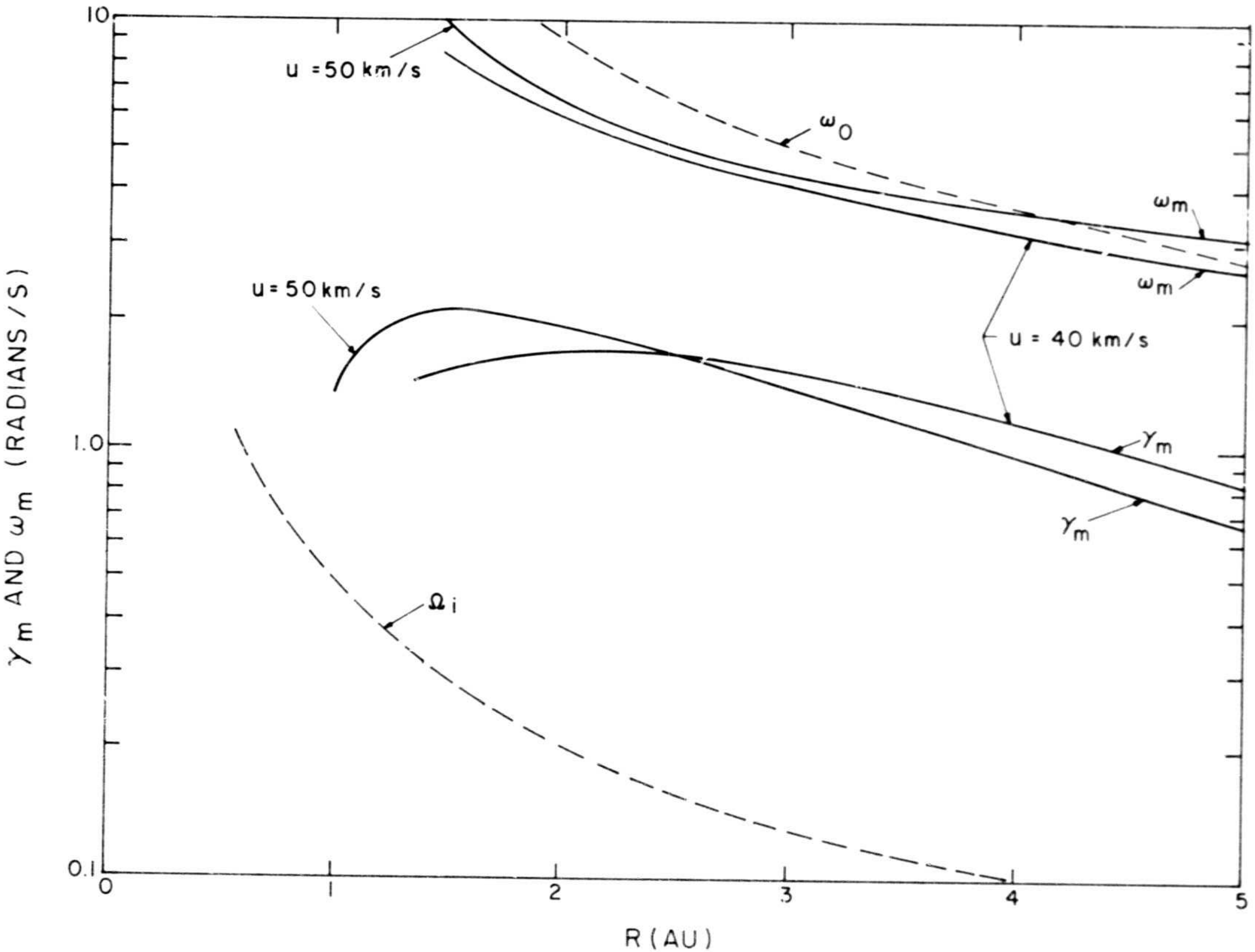

10
1.0
0.1
0
1
2
3
4
5
u = 50 km/s
u = 50 km/s
u = 40 km/s
ω_0
ω_m
ω_m
γ_m
γ_m
Ω_i
γ_m AND ω_m (RADIANS / S)
R (AU)

Figure 4

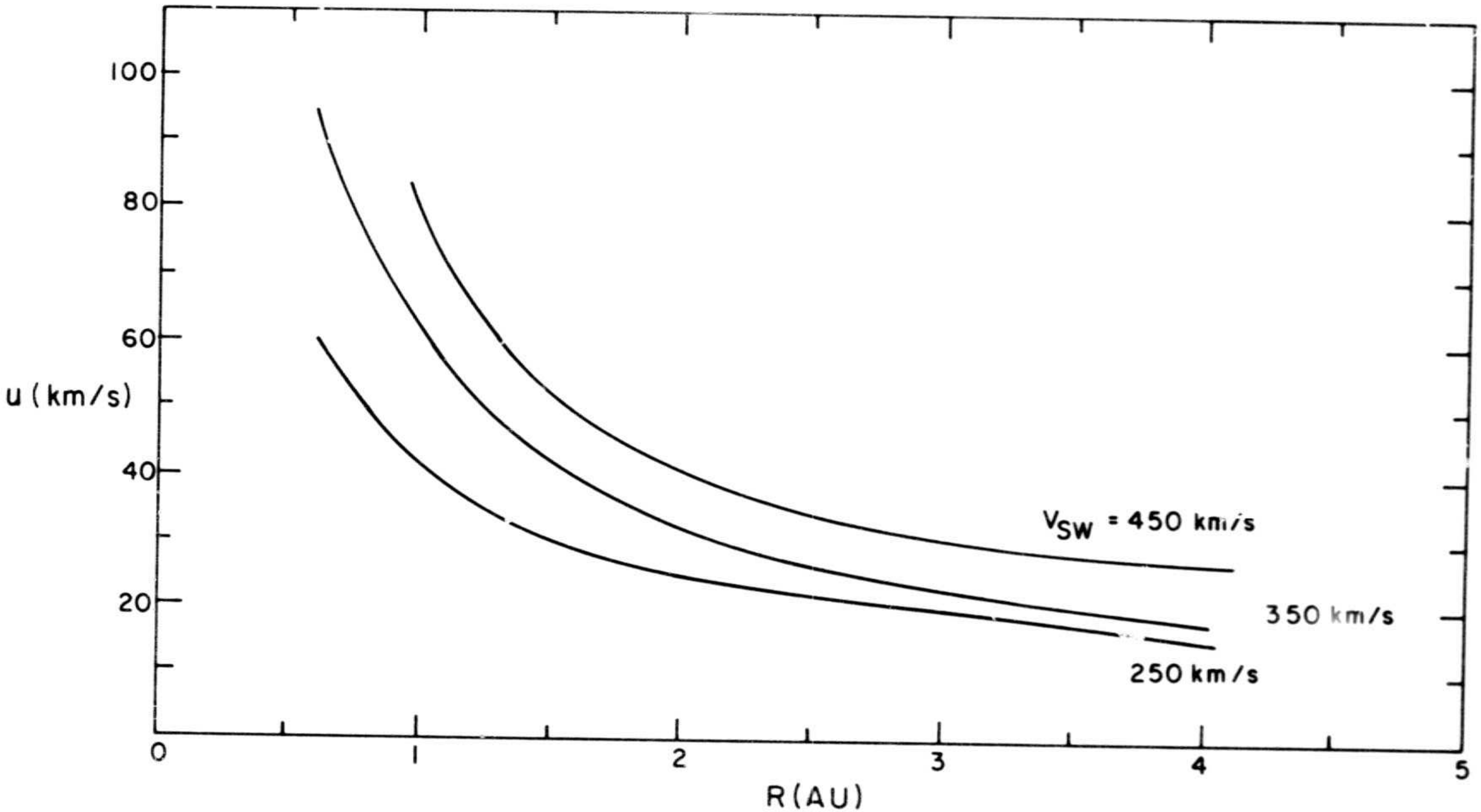

Figure 5

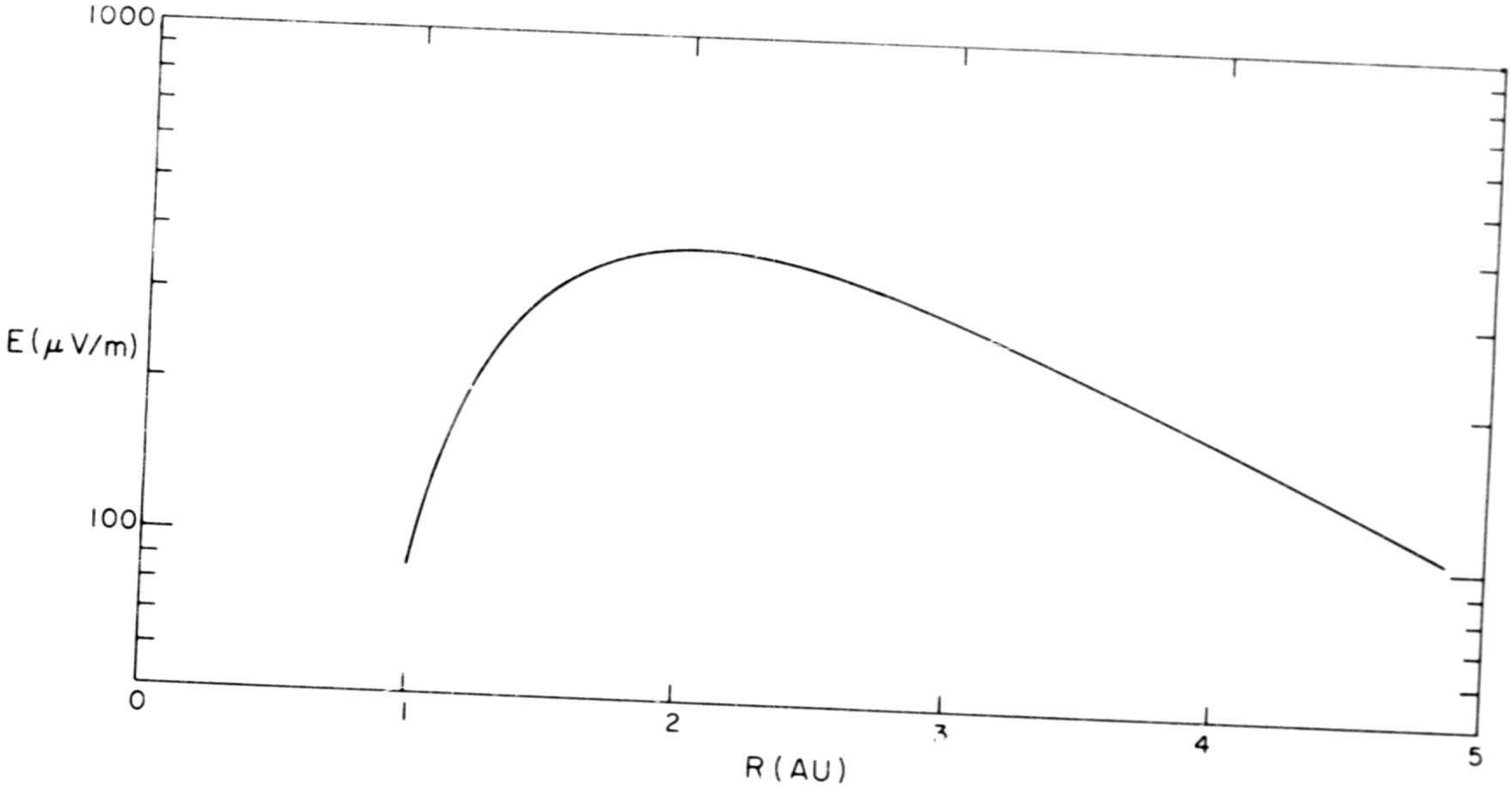

Figure 6

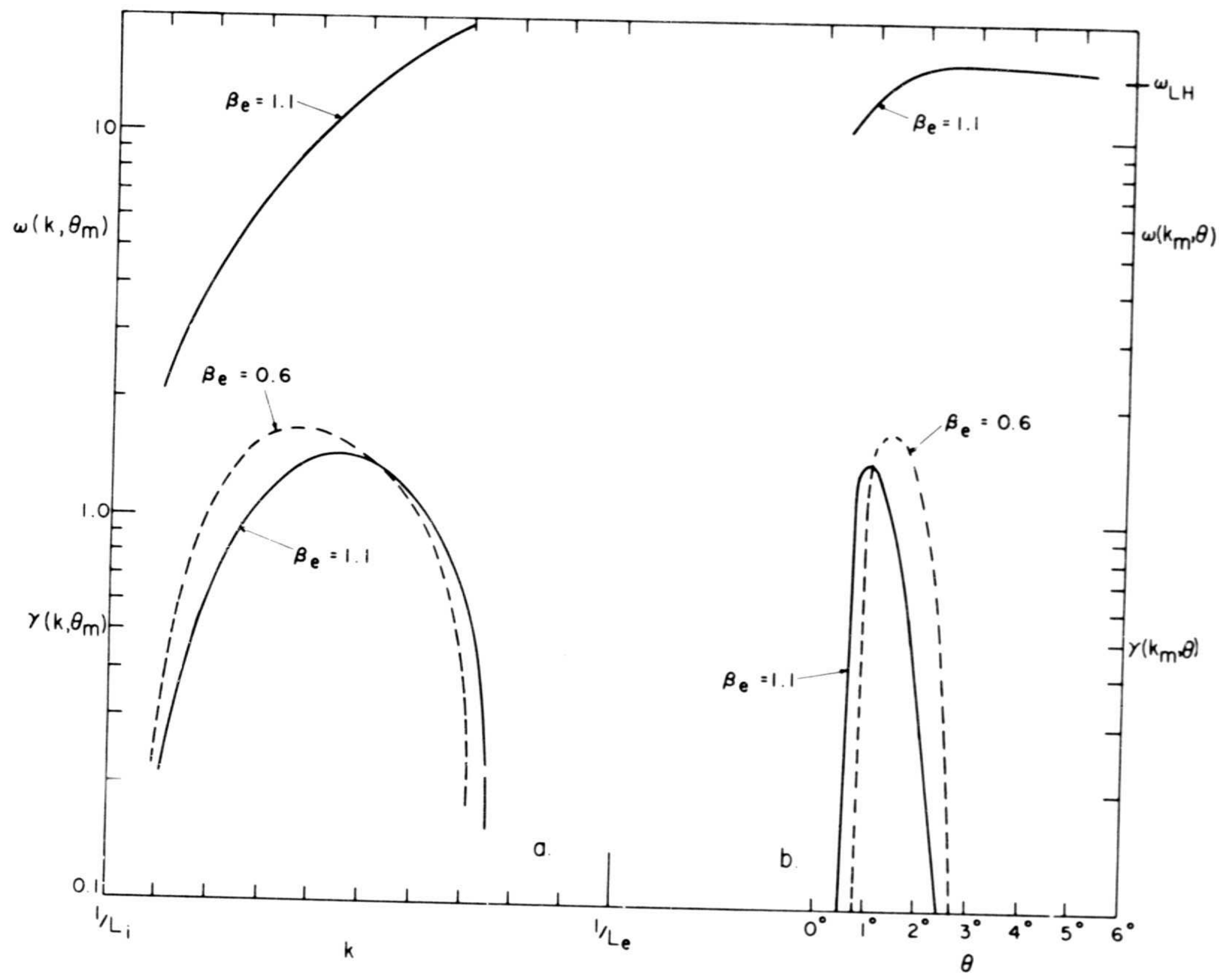

ω(k,θm)
γ(k,θm)
ω(km,θ)
γ(km,θ)
ωLH
βe = 1.1
βe = 0.6
βe = 1.1
βe = 1.1
βe = 0.6
βe = 1.1
10
1.0
0.1
1/Li
k
1/Le
a.
b.
0° 1° 2° 3° 4° 5° 6°
θ

Figure 7

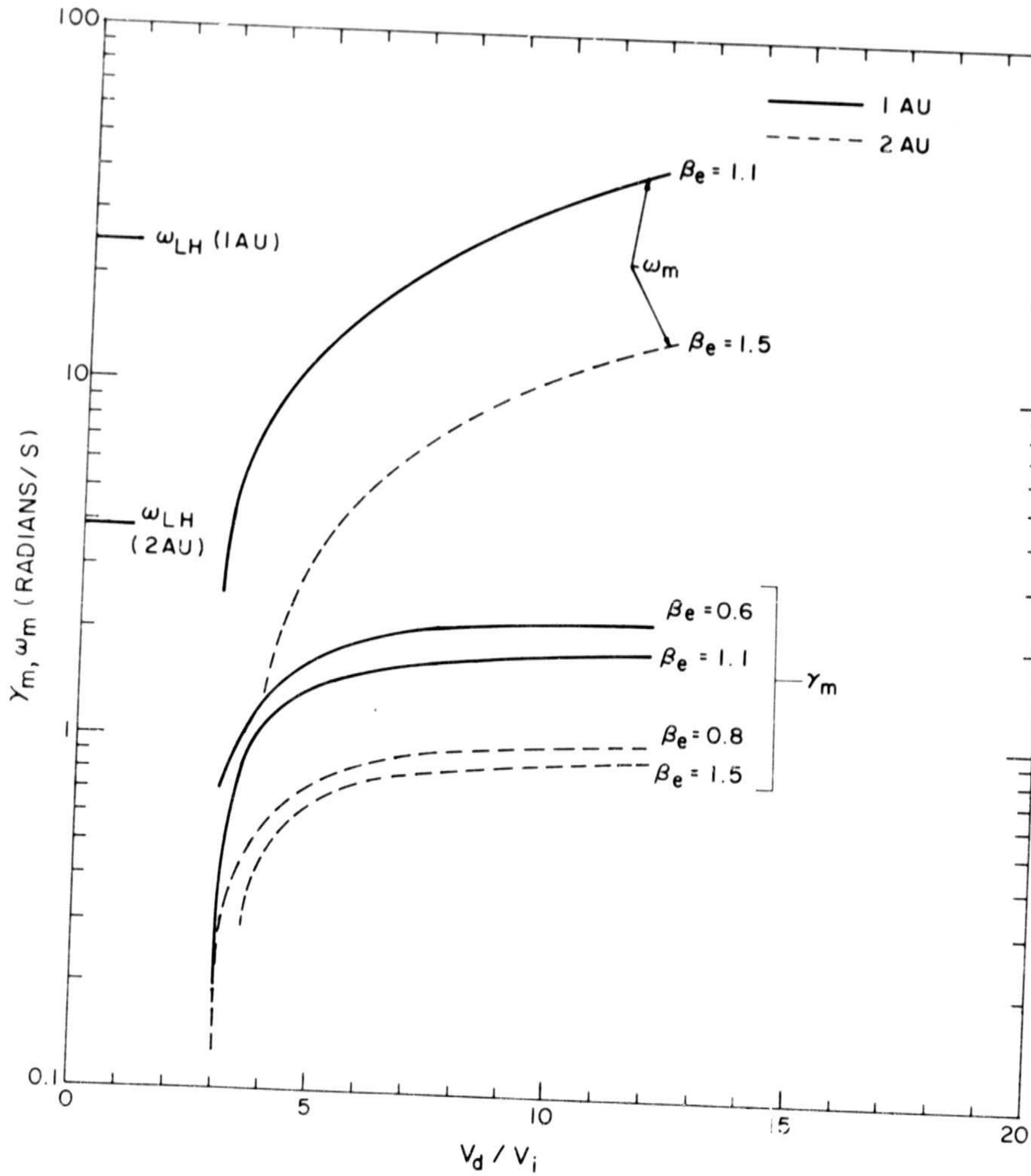

1 AU
2 AU
$\beta_e = 1.1$
ω_m
$\beta_e = 1.5$
ω_{LH} (1AU)
ω_{LH} (2AU)
$\beta_e = 0.6$
$\beta_e = 1.1$
γ_m
$\beta_e = 0.8$
$\beta_e = 1.5$
γ_m, ω_m (RADIANS/S)
V_d / V_i
100
10
1
0.1
0
5
10
15
20

Figure 8

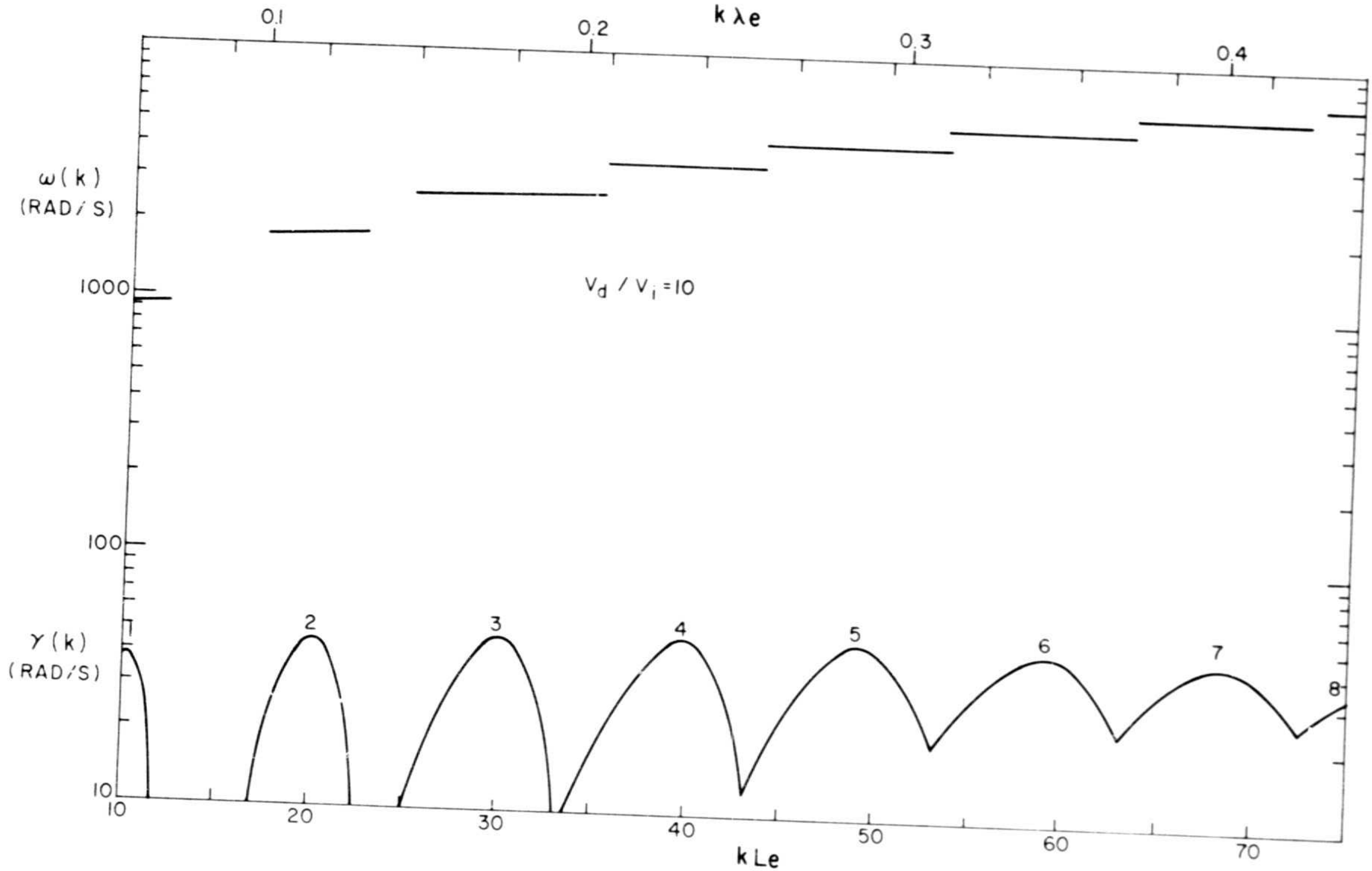
k λe
0.1
0.2
0.3
0.4
ω(k)
(RAD/S)
1000
100
γ(k)
(RAD/S)
10
Vd / Vi = 10
1
2
3
4
5
6
7
8
10
20
30
40
50
60
70
k Le

Figure 9

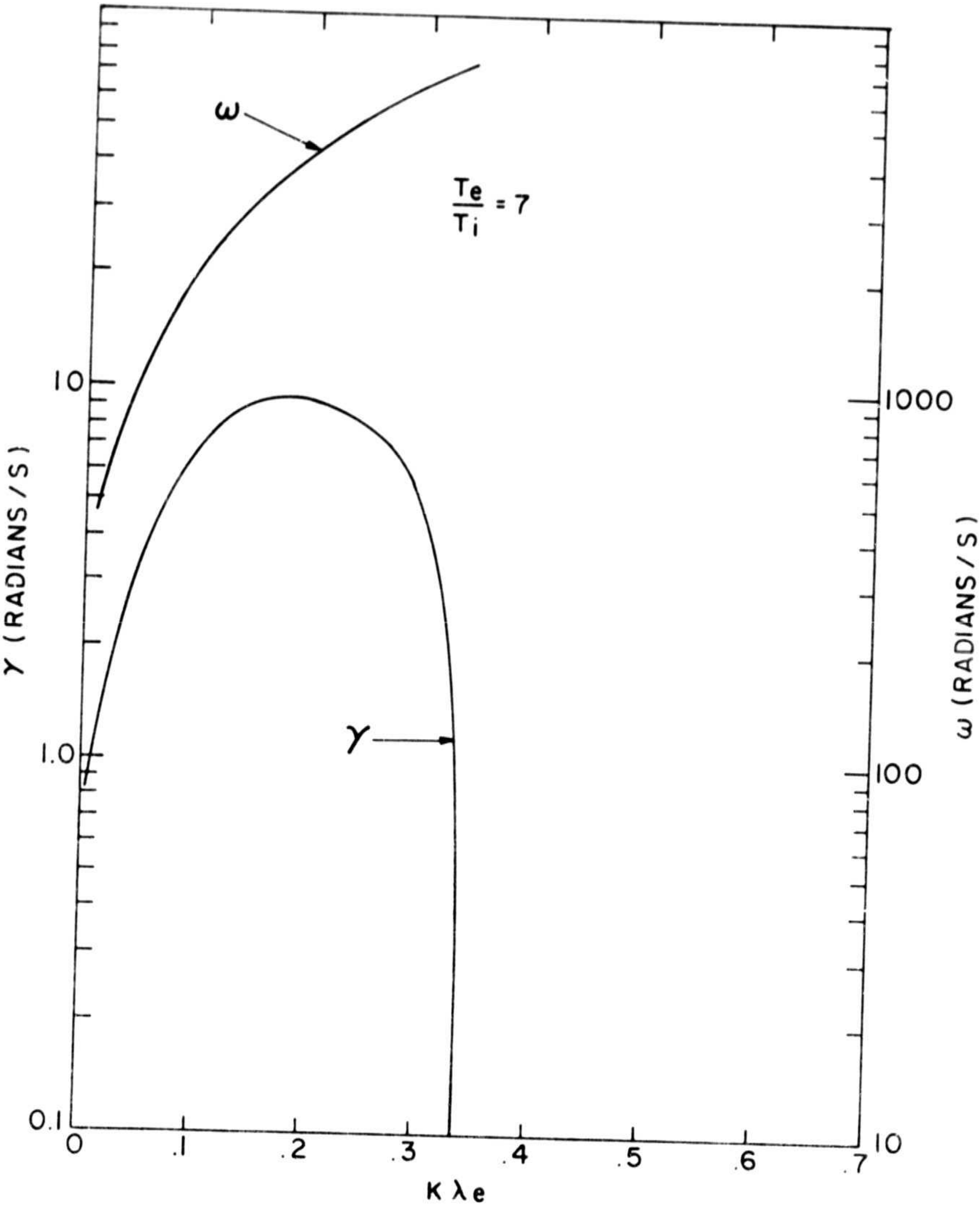
ω
γ
$\frac{T_e}{T_i} = 7$
γ (RADIANS / S)
ω (RADIANS / S)
0.1
1.0
10
10
100
1000
0
.1
.2
.3
.4
.5
.6
.7
κ λe

Figure 10